Published OnlineFirst December 5, 2011; DOI: 10.1158/1535-7163.MCT-11-0755

Preclinical Development

Molecular Cancer Therapeutics

Ganetespib, a Unique Triazolone-Containing Hsp90 Inhibitor, Exhibits Potent Antitumor Activity and a Superior Safety Profile for Cancer Therapy

Weiwen Ying, Zhenjian Du, Lijun Sun, Kevin P. Foley, David A. Proia, Ronald K. Blackman, Dan Zhou, Takayo Inoue, Noriaki Tatsuta, Jim Sang, Shuxia Ye, Jamie Acquaviva, Luisa Shin Ogawa, Yumiko Wada, James Barsoum, and Keizo Koya

Abstract

Targeted inhibition of the molecular chaperone Hsp90 results in the simultaneous blockade of multiple oncogenic signaling pathways and has, thus, emerged as an attractive strategy for the development of novel cancer therapeutics. Ganetespib (formerly known as STA-9090) is a unique resorcinolic triazolone inhibitor of Hsp90 that is currently in clinical trials for a number of human cancers. In the present study, we showed that ganetespib exhibits potent *in vitro* cytotoxicity in a range of solid and hematologic tumor cell lines, including those that express mutated kinases that confer resistance to small-molecule tyrosine kinase inhibitors. Ganetespib treatment rapidly induced the degradation of known Hsp90 client proteins, displayed superior potency to the ansamycin inhibitor 17-allylamino-17-demethoxygeldanamycin (17-AAG), and exhibited sustained activity even with short exposure times. *In vivo*, ganetespib showed potent antitumor efficacy in solid and hematologic xenograft models of oncogene addiction, as evidenced by significant growth inhibition and/or regressions. Notably, evaluation of the microregional activity of ganetespib in tumor xenografts showed that ganetespib was efficiently distributed throughout tumor tissue, including hypoxic regions >150 μm from the microvasculature, to inhibit proliferation and induce apoptosis. Importantly, ganetespib showed no evidence of cardiac or liver toxicity. Taken together, this preclinical activity profile indicates that ganetespib may have broad application for a variety of human malignancies, and with select mechanistic and safety advantages over other first- and second-generation Hsp90 inhibitors. *Mol Cancer Ther; 11(2); 475–84. ©2011 AACR.*

Introduction

Hsp90 is a molecular chaperone that regulates the posttranslational folding, stability and function of its protein substrates (client proteins), many of which play critical roles in cell growth, differentiation, and survival (1, 2). As with other physiologic processes that become coopted by tumor cells, it is now clear that the chaperoning functions of Hsp90 can become subverted during tumorigenesis to facilitate malignant progression (1). The Hsp90 machinery serves as a biochemical buffer for a number of oncogenic signaling proteins causally implicated in a variety of tumors (3, 4). Often, these oncoproteins are expressed as mutant forms that are particularly reliant on Hsp90 for stability and function (5, 6). Cancer cells contain elevated levels of the active form of the Hsp90 complex relative to normal cells, and have been shown to be selectively sensitive to Hsp90 inhibition (7, 8). Moreover, a unique characteristic of targeting Hsp90 is that inhibition results in the combinatorial blockade of multiple signal transduction cascades, thereby potentially bypassing pathway redundancies often found in cancer cells (9–11). Thus, Hsp90 represents an attractive molecular target for the development of novel cancer therapeutics (4, 11, 12).

The first class of Hsp90 inhibitors to be characterized were the benzoquinone ansamycins, including geldanamycin and its derivatives 17-allylamino-17-demethoxygeldanamycin (17-AAG), and 17-dimethylaminoethylamino-17-demethoxygeldanamycin (17-DMAG; ref. 13). However, the clinical progression of this group has been hampered because of several drawbacks including poor solubility, formulation problems, potential multidrug efflux, and hepatotoxicity (13, 14). In addition, as single agents, these inhibitors have only shown modest efficacies in the clinical setting (15, 16), indicating that they may be most effective as combination therapies. In an effort to overcome these limitations, several second-generation synthetic Hsp90 inhibitors representing

Authors' Affiliation: Synta Pharmaceuticals Corp., Lexington, Massachusetts

Note: Supplementary data for this article are available at Molecular Cancer Therapeutics Online (http://mct.aacrjournals.org/).

Corresponding Author: Weiwen Ying, Synta Pharmaceuticals Corp., 45 Hartwell Avenue, Lexington, MA 02421. Phone: 781-541-7243; Fax: 781-274-8228; E-mail: wying@syntapharma.com

doi: 10.1158/1535-7163.MCT-11-0755

Published OnlineFirst December 5, 2011; DOI: 10.1158/1535-7163.MCT-11-0755

multiple drug classes are currently under development (17–23).

In this article, we describe the preclinical characterization of ganetespib (formerly known as STA-9090), a novel small-molecule inhibitor of Hsp90 with a unique triazolone-containing chemical structure. Key pharmacologic and biologic properties of ganetespib distinguish this compound from other first- and second-generation Hsp90 inhibitors with regard to potency, antitumor activity, and an improved safety profile resulting in a superior therapeutic index. Accordingly, ganetespib is currently being evaluated in multiple phase I and II clinical trials. Taken together, these results support the continued development of ganetespib as a novel therapeutic agent for a variety of human cancers.

Materials and Methods

Cell lines, antibodies, and reagents

All cell lines were obtained from the American Type Culture Collection (ATCC) and maintained according to standard techniques. The cell lines were authenticated by the routine ATCC Cell Biology Program using short tandem repeat analysis (DNA profiling) and were used within 6 months of receipt for this study. All primary antibodies were purchased from Cell Signaling Technology. Ganetespib [3-(2,4-dihydroxy-5-isopropylphenyl)-4-(1-methyl-1*H*-indol-5-yl)-1*H*-1,2,4-triazol-5(4*H*)-one] was synthesized by Synta Pharmaceuticals Corp. 17-AAG, 17-DMAG, and erlotinib were purchased from LC Laboratories. Purified Hsp90 protein was obtained from Stressgen and recombinant human hepatocyte growth factor (HGF) from R&D Systems.

Cell viability assays

Cells were grown in 96-well plates based on optimal growth rates determined empirically for each line. Twenty-four hours after plating, cells were treated with the indicated compounds or controls for 72 hours. AlamarBlue (Invitrogen) was added (10% v/v) to the cells, and the plates were incubated for 3 hours and, then, subjected to fluorescence detection. For the comparative viability/apoptosis assay, NCI-H1975 cells were treated with escalating concentrations of ganetespib for the indicated time periods and subjected to viability analysis via CellTiter Fluor (Promega) and apoptosis via Caspase Glo 3/7 (Promega).

Western blotting

Following treatment, tumor cells were disrupted in lysis buffer (CST) on ice for 10 minutes. Lysates were clarified by centrifugation and equal amounts of proteins resolved by SDS-PAGE before transfer to nitrocellulose membranes (Invitrogen). Membranes were blocked with 5% skim milk in Tris-buffered saline with 0.5% Tween and immunoblotted with the indicated antibodies. The antibody–antigen complex was visualized and quantitated using an Odyssey system (LI-COR).

In vivo xenograft tumor models

Female immunodeficient Crl:CD1-*Foxn1*^{nu} (nude) and CB-17/Icr-*Prkdc*^{scid}/Crl severe combined immunodeficient (SCID) mice (Charles River Laboratories) were maintained in a pathogen-free environment, and all *in vivo* procedures were approved by the Institutional Animal Care and Use Committee of Synta Pharmaceuticals Corp. NCI-H1395 and MV4-11 cells were subcutaneously implanted into SCID mice and MKN45 cells into nude mice. Mice bearing established tumors (100–200 mm^3) were randomized into treatment groups of 8 and intravenously dosed via the tail vein with either vehicle or ganetespib formulated in 10/18 DRD (10% dimethyl sulfoxide, 18% Cremophor RH 40, 3.6% dextrose, 68.4% water). In the NCI-H1395 model, studies were conducted at the highest nonseverely toxic doses of 150 mg/kg weekly; in the MV4-11 model, animals were treated with ganetespib at 100 and 125 mg/kg weekly; in the MKN45 model, animals were treated with ganetespib at 50 mg/kg 3 times a week. Tumor growth inhibition was determined as described previously (24).

Microregional activity of ganetespib in NCI-H1975 xenografts

NCI-H1975 tumor xenograft-implanted SCID mice were treated with 125 mg/kg ganetespib for 6 to 72 hours. At the end of the experiment, mice were administered bromodeoxyuridine (BrdUrd) and pimonidazole to label S-phase cells and hypoxic tumor regions and, then 5 minutes before excision, mice were administered $DiOC_7(3)$ to demarcate perfused vessels. Following tumor excision and freezing, 10-μm thick cryosections were cut and sequentially immunostained to detect markers of proliferation (BrdUrd), apoptosis (TUNEL), hypoxia (HIF-1α), and tumor vasculature (CD31). Images of CD31 fluorescence, BrdUrd, and terminal deoxynucleotidyl transferase–mediated dUTP nick-end labeling (TUNEL) staining from each section were overlaid, and areas of necrosis and staining artifacts were manually removed. Proliferation and apoptosis were plotted as a function of distance from vessels.

Hepatotoxicity assay

Male Sprague–Dawley rats were treated with repeated daily administration of escalating doses of 17-DMAG (formulated in 5% dextrose in water) or ganetespib (formulated in DRD). Blood serum was collected during necropsy at the end of the experiment in all rats treated with or without testing compound. The serum liver enzyme tests were conducted at IDEXX Laboratories according to their validated standard operation procedure. For histologic analysis, livers were removed at necropsy and formalin fixed. Paraffin-embedded sections were processed and stained with hematoxylin and eosin for routine histologic evaluation.

Published OnlineFirst December 5, 2011; DOI: 10.1158/1535-7163.MCT-11-0755

Langendorff assay

Briefly, hearts from male New Zealand white rabbits were used to measure the physiologic variables PQ, QRS, RR, QT, and dLVP/dt following perfusion with escalating doses of ganetespib (10^{-8}–10^{-4} mmol/L; see Supplementary Materials and Methods for complete details). Mean values for each parameter were calculated for each concentration, and mean values (±SEM) were plotted against concentration for all parameters assessed, both for ganetespib-exposed and vehicle-treated hearts.

Results

Ganetespib binds to the N-terminal ATP-binding site in Hsp90

Ganetespib is a novel resorcinolic triazolone compound that is structurally distinct to the first-generation ansamycin Hsp90 inhibitors. The chemical structure is shown in Fig. 1A. With a molecular weight of 364.4, ganetespib is considerably smaller than the ansamycin class, and most of the newer, second-generation Hsp90 inhibitors. Ganetespib is relatively hydrophobic, with a cLogP value of 3.3. Ganetespib exhibits competitive binding for the ATP pocket at the N-terminus of Hsp90. There are reports that the N-terminus can be crystallized in a number of conformations including an open or closed conformation in reference to the position of the ATP-binding pocket lid (25). We have obtained the co-crystal structure of ganetespib bound to the closed conformation of the Hsp90 N-terminus (Fig. 1B); however, we anticipate that ganetespib can also access the ATP pocket in the open conformation based on computational analysis (data not shown).

The X-ray co-crystal structure of ganetespib bound to Hsp90 (Fig. 1C) confirmed important hydrogen bonding interactions, also seen in the ansamycin family, involving the resorcinol hydroxyl group with Asp^{93} and the carbonyl group of triazolone with Lys^{58}. Importantly, in ganetespib, the 2-hydroxyl of resorcinol is within hydrogen bonding distance to both oxygen atoms of the carboxylic group in Asp^{93}, resulting in a substantially stronger interaction. Furthermore, the N^2 of triazolone forms a water-bridged hydrogen bond with Asp^{93} to provide additional hydrogen bonding. Water-bridge hydrogen bonds between 4-hydroxyl of resorcinol and Leu^{48} and Ser^{52} were found to be critical for binding efficiency in our optimization efforts. The hydrazinecarboxamide moiety of triazolone in ganetespib is of particular structural importance. In addition to the direct hydrogen bond with Lys^{58}, it forms a unique hydrogen bond with Gly^{97}, a distinguishing feature from the ansamycin analogues. Furthermore, it interacts with Thr^{184} and Asp^{102} through water-bridge hydrogen bonding (Fig. 1C).

Ganetespib displays superior potency to 17-AAG in a broad range of tumor cells

The *in vitro* cytotoxic activity of ganetespib was determined against a panel of 57 transformed cell lines derived from both hematologic and solid tumors and compared with that of 17-AAG (Supplementary Table S1). Ganetespib was potently cytotoxic in the majority of the lines examined, typically with IC_{50} values in the low nanomolar range. Overall, ganetespib showed a 20-fold greater potency than 17-AAG with median IC_{50} values of 14 versus 280 nmol/L, respectively. This difference in sensitivity was more significantly pronounced in the subset of hematologic malignancies, which showed a 47.5-fold difference (median IC_{50} values of 10 vs. 475 nmol/L). Indeed, leukemic cell lines [acute myeloid leukemia (AML), chronic myeloid leukemia (CML), B-cell lymphoma, and anaplastic large-cell lymphoma (ALCL)] manifested the greatest sensitivity to ganetespib treatment, whereas melanoma and prostate cancer represented tumor types in which ganetespib was also highly cytotoxic (Supplementary Table S1). Notably, ganetespib retained potency against cell lines expressing mutated kinases that confer resistance to kinase inhibitors that are currently used in clinical practice.

Ganetespib induces cell-cycle arrest and apoptosis

Cell-cycle analysis showed that ganetespib induced marked accumulation in the G_2–M phase within 24 hours in NCI-H1975 cells, with a concomitant loss of S phase (Supplementary Fig. S1). The viable cell population remained blocked for at least 72 hours; however, over this period, the percentage of apoptotic cells increased. To confirm this, cells were exposed to increasing concentrations of ganetespib for 6 to 72 hours. Apoptosis was

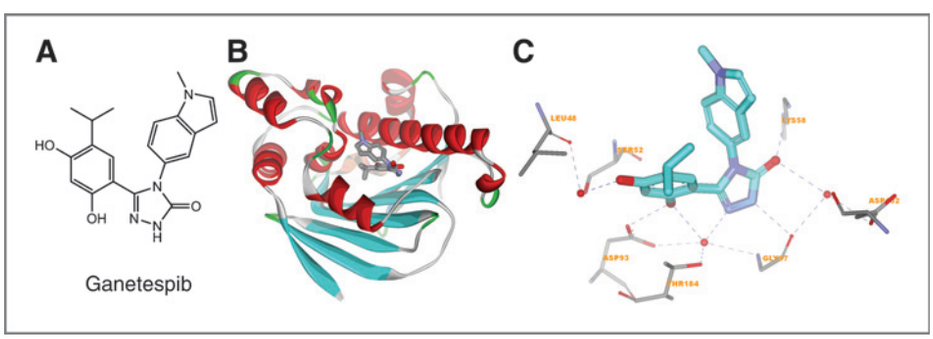

Figure 1. Chemical structure of ganetespib and its co-crystal structure with Hsp90 N-terminal. A, chemical structure of ganetespib. B, crystallographic complex of ganetespib in the Hsp90 N-terminal. C, hydrogen bond interactions between ganetespib with amino acid residues in the Hsp90 N-terminal ATP-binding pocket.

Published OnlineFirst December 5, 2011; DOI: 10.1158/1535-7163.MCT-11-0755

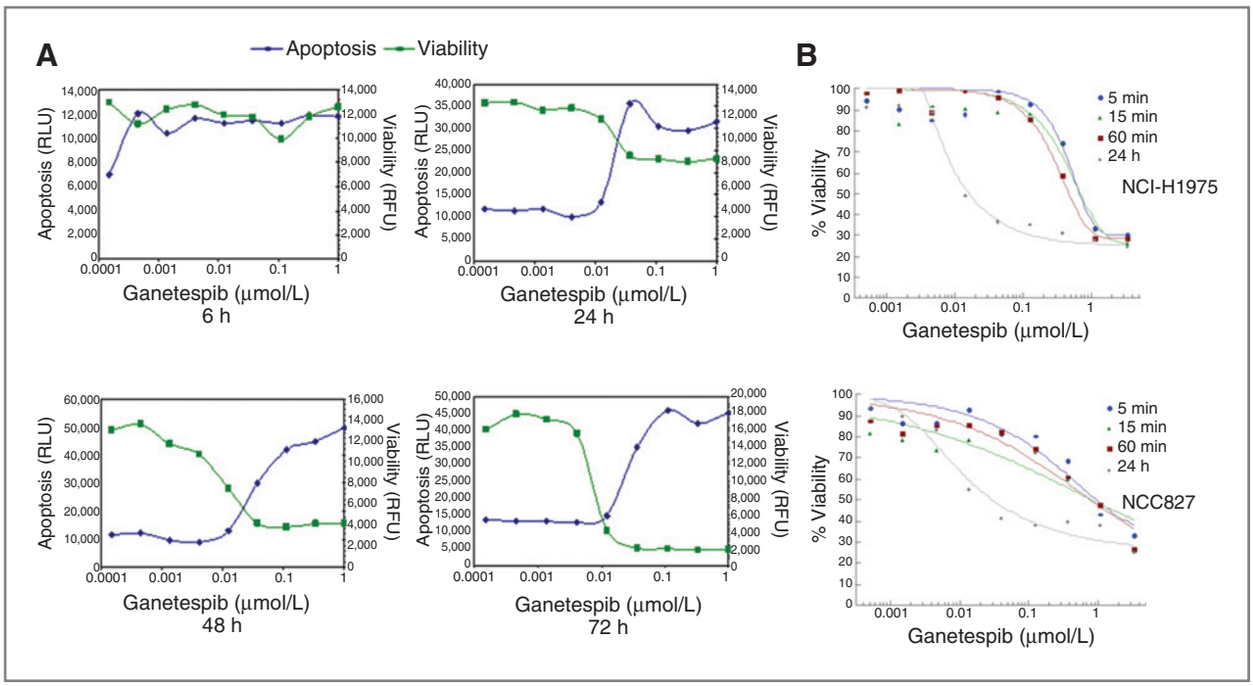

Figure 2. Ganetespib induces apoptosis in human cancer cells *in vitro*. A, NCI-H1975 cells were treated with increasing concentrations of ganetespib for 6, 24, 48, and 72 hours and then subjected to analysis of viability and apoptosis. The IC_{50} values for viability at 6, 24, 48, and 72 hours were >1,000, >1,000, 16, and 8 nmol/L, respectively. B, NCI-H1975 and HCC827 cells were exposed to graded concentrations of ganetespib for 5, 15, and 60 minutes and 24 hours. Cell viability was assessed 72 hours following drug wash-out. RFU, relative fluorescence units.

measured using activated caspase 3/7 levels and compared with cell viability (Fig. 2A). No effects were seen 6 hours after treatment. However, the marked loss of viability following exposure to ganetespib observed 24 to 48 hours posttreatment correlated with increased apoptotic induction. These results indicate that ganetespib-induced cytotoxicity is mediated by an irreversible commitment to apoptosis, which is likely subsequent to growth arrest and effects on the cell cycle (24).

Ganetespib exhibits sustained activity with short exposure times

We then investigated the exposure time of ganetespib required to induce cytotoxic responses *in vitro* using the NCI-H1975 and HCC827 non–small cell lung carcinoma (NSCLC) lines. Cells were exposed to ganetespib for the indicated times (5, 15, and 60 minutes and 24 hours), washed to remove the drug, and then grown in standard medium until cell viability was measured at 72 hours (Fig. 2B). Unexpectedly, exposure to ganetespib for only 60 minutes resulted in cytotoxicity with IC_{50} values of 510 and 800 nmol/L for NCI-H1975 and HCC827 cells, respectively (Supplementary Table S2). Remarkably, a 5-minute exposure to ganetespib in NCI-H1975 cells still resulted in an IC_{50} value < 1 μmol/L, a plasma concentration that is achievable *in vivo*. These findings indicated that cell viability was quickly affected by ganetespib treatment and indicate that even brief drug exposure may be sufficient to affect tumor growth.

Ganetespib displays potent activity against drug-resistant tumor phenotypes *in vitro*

In NSCLC, activating mutations in epidermal growth factor receptor (EGFR) can drive tumorigenesis and confer sensitivity to tyrosine kinase inhibitors (TKI) such as erlotinib and gefitinib (26). To examine whether ganetespib could overcome the resistant phenotype in NSCLC cells, we compared the activities of ganetespib and erlotinib (Supplementary Fig. S2) using the NCI-H1975 cell line, which expresses a mutationally activated and erlotinib-resistant $EGFR^{L858R/T790M}$ mutation, and the erlotinib-sensitive HCC827 cells, which express $EGFR^{Del\ E746\_A750}$ (Fig. 3A). As expected, erlotinib treatment resulted in dose-dependent cytotoxicity in HCC827 cells, but had no effect on NCI-H1975 cells. In contrast, ganetespib exhibited full potency against both cell lines, irrespective of EGFR mutational status.

In addition, resistance to EGFR inhibitors may emerge through alternative oncogenic mechanisms. HGF, a ligand of the c-MET oncoprotein, can induce TKI resistance in lung tumors with EGFR-activating mutations by independently activating and restoring phosphoinositide 3-kinase (PI3K)–AKT signaling via phosphorylation of c-MET (27, 28). Given that EGFR, c-MET, and AKT are all Hsp90 client proteins, we, therefore, determined whether ganetespib was active against c-MET–induced TKI-resistant cells. HCC827 cells were seeded in the presence or absence of HGF (50 ng/mL) and, 24 hours later, were dosed with ganetespib or erlotinib. Cell viability was assessed 72 hours after addition of the drug (Fig. 3B).

Published OnlineFirst December 5, 2011; DOI: 10.1158/1535-7163.MCT-11-0755

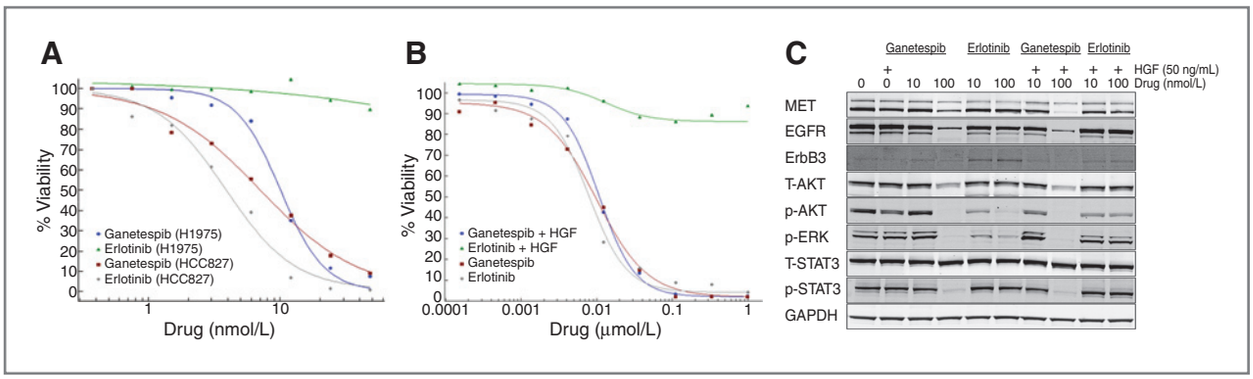

Figure 3. Ganetespib exhibits potency against erlotinib-resistant NSCLC tumor phenotypes *in vitro*. A, NCI-H1975 and HCC827 cells were treated with increasing concentrations of ganetespib or erlotinib and cell viability was assessed after 72 hours. B, HCC827 cells were seeded in the presence or absence of HGF (50 ng/mL) for 24 hours, then exposed to graded concentrations of ganetespib or erlotinib for 72 hours. Cell viability was measured by AlamarBlue. C, HCC827 cells seeded with or without 50 ng/mL HGF for 24 hours were treated with 0, 10, or 100 nmol/L ganetespib or erlotinib for an additional 24 hours. The levels of MET, EGFR, ErbB3, total (T-) AKT, p-AKT, p-ERK1/2, and GAPDH were subjected to Western blot analysis. GAPDH, glyceraldehyde-3-phosphate dehydrogenase.

Both ganetespib and erlotinib were highly potent in non-stimulated HCC827 cells, with IC_{50} values of approximately 10 nmol/L. Importantly, whereas HGF-treated cells did not respond to erlotinib, ganetespib retained its potency in the presence of the growth factor. Similar results were observed in HCC827 cells selected for *MET* amplification (data not shown)

To examine modulation of MET-driven AKT signaling by ganetespib, HCC827 cells seeded with or without HGF for 24 hours were treated with ganetespib or erlotinib at either 10 or 100 nmol/L doses (which represent the IC_{50} and IC_{100} drug concentrations, respectively). Cells were harvested at 24 hours, and levels of MET, EGFR, and their relevant effectors were examined by Western blot analysis (Fig. 3C). Ganetespib treatment promoted the downregulation of MET, EGFR, and AKT protein levels in both the absence and presence of HGF, resulting in the complete loss of AKT and extracellular signal-regulated kinase (ERK) activity. Erlotinib exposure was capable of inactivating AKT and ERK in the absence of HGF, but was ineffective in the presence of the growth factor.

Ganetespib exhibits potent *in vivo* activity in both solid and hematologic xenograft models

To determine whether the effects of ganetespib *in vitro* translate to antitumor efficacy *in vivo*, the activity of ganetespib was evaluated using a variety of doses and schedules in a series of xenograft models. Initially, SCID mice bearing NCI-H1395 NSCLC xenografts were dosed intravenously with ganetespib on a weekly schedule at its highest nonseverely toxic dose of 150 mg/kg (Fig. 4A). NCI-H1395 tumor regression was induced by ganetespib with a T/C value of −49% compared with the control group. Importantly, this regimen was well tolerated with minimal loss of body weight observed during the course of treatment (Fig. 4B).

MV4-11 AML cells express the Hsp90 client protein FLT3, an oncogenic driver and the most common genetic alteration associated with AML (29). This cell line is highly sensitive to ganetespib *in vitro* (IC_{50}: 4 nmol/L; Supplementary Table S1). Ganetespib was administered intravenously to MV4-11 tumor–bearing SCID mice once weekly at 100 and 125 mg/kg. As shown in Fig. 4C, these 2 treatment regimens resulted in significant tumor regression (85% and 94%, respectively). Moreover, tumors were undetectable in 37.5% of ganetespib-treated animals at the end of the 3-week dosing period.

Amplification of the c-MET receptor tyrosine kinase occurs in approximately 20% of gastric carcinomas (30). We, therefore, used the human c-MET amplified MKN45 gastric carcinoma cell line as an additional xenograft model of oncogene addiction to examine the antitumor activity of ganetespib (Fig. 4D). Ganetespib treatment was again highly efficacious in this study, with a 50 mg/kg dose 3 times per week resulting in 92% inhibition of tumor growth.

Ganetespib penetrates hypoxic regions of tumors *in vivo*

To evaluate tumor penetration, the microregional activity of ganetespib was assessed in NCI-H1975 tumor xenografts. Immunohistochemical markers of proliferation (BrdUrd), apoptosis (TUNEL), and hypoxia (HIF-1α) in tumors were mapped in relation to distance from the nearest $CD31^+$ endothelial cells (Fig. 5). A single dose of ganetespib at 125 mg/kg dramatically reduced cellular proliferation throughout the tumors, with the maximal effect occurring 24 hours following treatment (Fig. 5A). Furthermore, a concomitant induction of tumor cell apoptosis occurred within 24 hours (Fig. 5B). Moreover, at 6 hours, apoptosis was preferentially induced near vessels and then became uniformly induced throughout the tissue by the 48-hour time point (data not shown). Increased HIF-1α staining as a function of distance confirmed the hypoxic gradient that existed within the tumors and, importantly, this Hsp90 client protein was potently

Published OnlineFirst December 5, 2011; DOI: 10.1158/1535-7163.MCT-11-0755

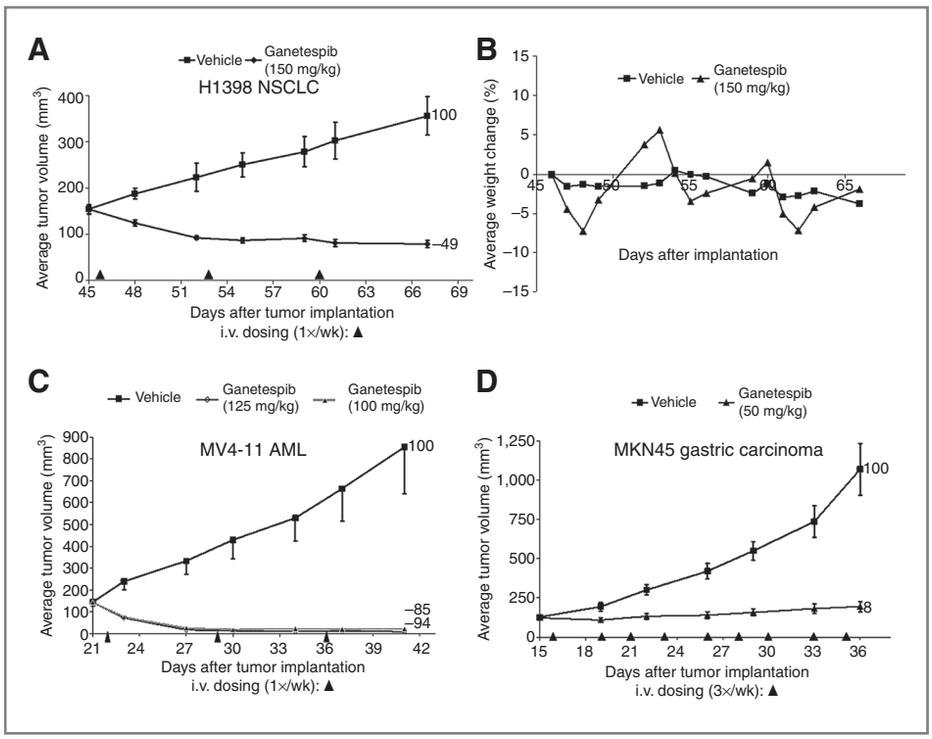

Figure 4. Ganetespib exhibits potent antitumor efficacy in oncogene-driven xenograft models of solid and hematologic malignancies. Xenografts: 100–200 mm^3; $n = 8$ mice per group. The % T/C values are indicated to the right of each growth curve and the error bars are the SEM. A, mice bearing established NCI-H1395 xenografts were intravenously dosed with ganetespib at 150 mg/kg once weekly as indicated (arrowheads). B, body weights were measured 5 times per week. Mean values are plotted against vehicle controls. C, mice bearing established MV4-11 xenografts were intravenously dosed with ganetespib at 100 and 125 mg weekly as indicated (arrowheads). D, mice bearing established MKN45 xenografts were intravenously dosed with ganetespib at 50 mg/kg 3 times per week as indicated (arrowheads).

suppressed *in vivo* following treatment with ganetespib (Fig. 5C). These results provide strong evidence that ganetespib efficiently distributed within the extravascular compartment, including the hypoxic regions >150 μm from the microvasculature, resulting in sustained inhibition of proliferation and induction of apoptosis throughout the tumors.

Ganetespib exhibits a favorable safety profile

The hepatotoxicity profile of ganetespib was evaluated in male Sprague–Dawley rats on the basis of changes in the liver enzymes aspartate aminotransferase (AST) and alanine aminotransferase (ALT; Fig. 6A). Animals were treated with repeated administration of ganetespib at 25, 50, and 75 mg/kg/d for 5 days, or 17-DMAG (Supplementary Fig. S2) at 2, 4, and 6 mg/kg/d for 4 days. No changes in the levels of either enzyme were observed in the ganetespib-treated animals, even at the highest dose of 75 mg/kg, which is higher than the efficacious dose range for this compound. A dose of 75 mg/kg represented the effective maximum tolerated dose in these animals, as extensive gastrointestinal toxicity was observed following the 5-day treatment. In stark contrast, a dose-dependent and marked elevation of ALT (293%–510%) and AST (149%–296%) was seen with 17-DMAG–treated rats, at doses 12.5 times lower than that of ganetespib. Histologic analysis (Fig. 6B) revealed that livers of animals treated with 17-DMAG at the lowest dose (2 mg/kg) showed patchy and focal hepatocytic apoptosis with mild mononuclear cell infiltration. At a dose of 6 mg/kg, the lesions were diffuse and severe, including larger areas of coagulative hepatocytic necrosis. These injuries were primarily observed in the area near the central vein of the hepatic plate and are consistent with the elevated levels of liver enzymes. In accordance with the lack of enzymatic induction, there were no discernable morphologic changes in the hepatocytes of animals treated with ganetespib.

Cardiovascular effects of escalating doses ganetespib on electrophysiologic (PQ, QRS, RR, and QTc) and mechanical (left ventricular developed pressure) properties were evaluated in isolated New Zealand white rabbit hearts. Ganetespib exerted no significant physiologic effects other than a minimal reduction in atrioventricular conduction (lengthening PQ interval) and a minor reduction in heart rate (increased RR interval) over the concentrations 10^{-8} to 10^{-5} mol/L (data not shown). There was no change in the QTc(F) intervals at concentrations of ganetespib between 10^{-8} and 10^{-5} mol/L when compared with baseline or vehicle (Fig. 6C). Similarly, there was no change in the QRS duration after exposure to concentrations of ganetespib ranging from 10^{-8} to 10^{-6} mol/L, when compared with baseline or vehicle; however, an increase in the duration of the QRS was noted after exposure to the 10^{-5} mol/L concentration (Fig. 6C). At 10^{-4} mol/L, the highest concentration tested, ganetespib caused lengthening of PQ interval and QRS duration; however, this concentration was approximately 3,000-fold higher than the unbound C_{max} in the 125 mg/kg dose in the NCI-H1975 tumor-penetration studies (Fig. 5). Other cardiac electrophysiologic parameters and mechanical properties, including left ventricular developed pressure, were not significantly altered following exposure to

Published OnlineFirst December 5, 2011; DOI: 10.1158/1535-7163.MCT-11-0755

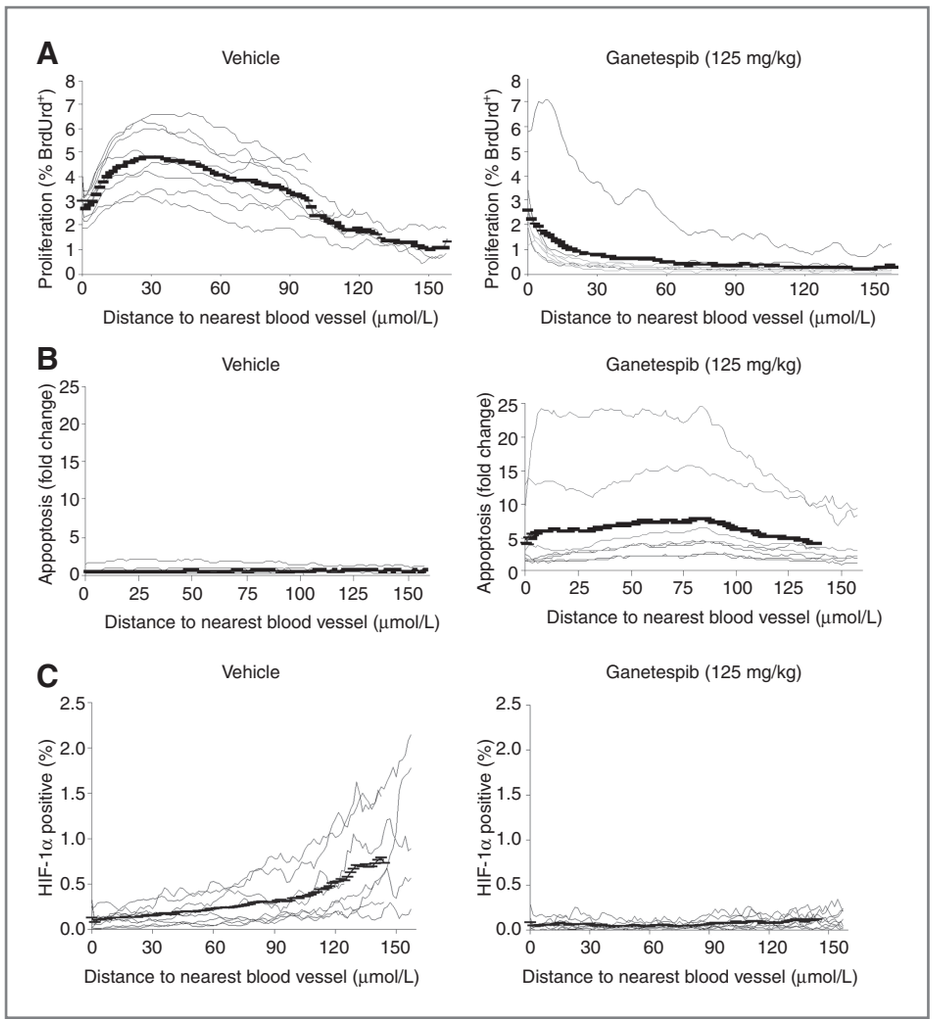

Figure 5. Tumor penetration and microregional activity of ganetespib. A single 125 mg/kg dose of ganetespib was administered intravenously to established NCI-H1975 xenografts, and tumors ($n = 8$ per group) were removed 24 hours after treatment. Immunohistochemical staining and analysis were carried out on cryosections for markers of proliferation (bromodeoxyuridine) and apoptosis (TUNEL). A, proliferation was mapped in relation to distance from the nearest $CD31^+$ endothelial cells. All (100%) tumor cells were located <170 μm from the nearest blood vessels. B, apoptosis was mapped in relation to distance from the nearest $CD31^+$ cells. C, HIF-1α expression was mapped in relation to distance from the nearest $CD31^+$ cells.

ganetespib, whereas expected physiologic changes with the positive control quinidine were observed (data not shown).

Discussion

In this article, we provide the first preclinical characterization of ganetespib, a novel and potent inhibitor of Hsp90 that offers considerable promise as a new targeted cancer therapeutic agent. Structurally, ganetespib is distinct from the first-generation ansamycin Hsp90 inhibitors, with a unique scaffold that is considerably smaller than these geldanamycin analogues. Hsp90 chaperone activity is associated with an ATP-driven conformational change within the N-terminal domain (31, 32). Our data show that ganetespib is able to enter the ATP-binding pocket in the so-called closed conformation. In contrast, due to their larger size, the ansamycin analogues can only occupy the ATP-binding pocket in the open conformation. For clarity, this discussion of open and closed conformation of the Hsp90 N-terminal refers to the positioning of the ATP pocket lid, which is different from the open and closed concept in the Hsp90 chaperoning cycle involving dimerization (33). This lack of restriction for binding to the Hsp90 ATP pocket may be one of the reasons that ganetespib shows higher *in vitro* potency than the geldanamycin analogues. In addition, our structural analysis has identified a series of additional hydrogen bond interactions due to the presence of the triazolone moiety that predict for superior binding affinities between ganetespib and Hsp90, further distinguishing this compound from the geldanamycin class.

Human cancers are typically characterized by a variety of genetic alterations that collectively contribute to the transformed state; however, a subset is now believed to be dependent on single, definable oncogenic pathways for their genesis, proliferation, and/or survival. This phenomenon is known as oncogene addiction (34) and, because a large number of the addicting oncoproteins are known Hsp90 clients, this has important implications for the development of targeted therapeutics. The panel of solid and hematologic tumor lines found to be sensitive to

Published OnlineFirst December 5, 2011; DOI: 10.1158/1535-7163.MCT-11-0755

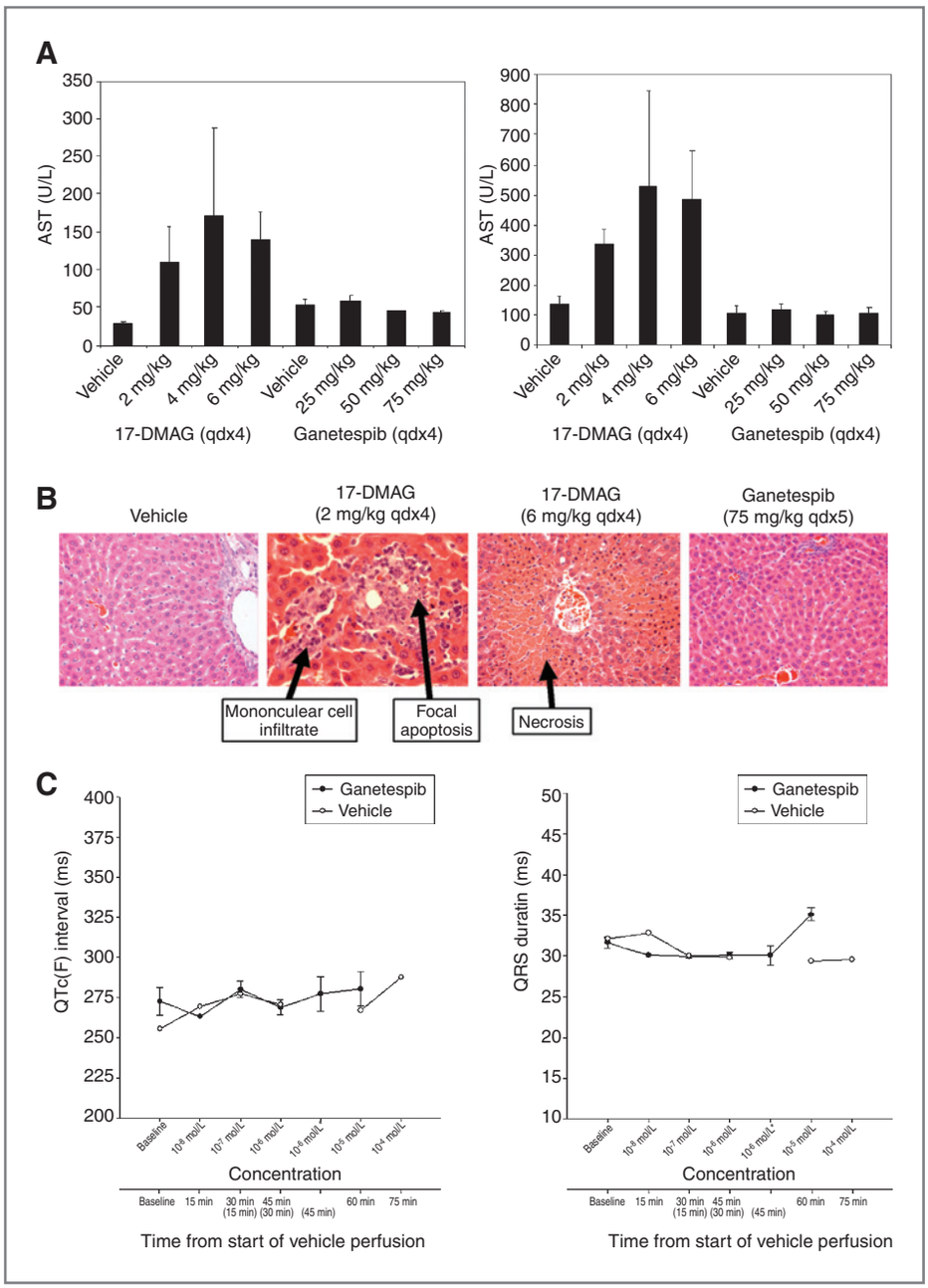

Figure 6. Liver and cardiovascular effects profile of ganetespib. A, male Sprague–Dawley rats ($n = 3$–5 rats per group) were treated with repeated administration of 17-DMAG at 2, 4, and 6 mg/kg for 4 days (qd $\times$ 4) or ganetespib at 25, 50, and 75 mg/kg for 5 days (qd $\times$ 5). Plasma levels of the liver enzymes aspartate aminotransferase (AST) and alanine aminotransferase (ALT) are presented. B, hematoxylin and eosin (H&E) staining of liver cross sections from vehicle control, 17-DMAG-, or ganetespib-treated animals. Original magnification, $\times$200 (second panel, $\times$400). C, effects of escalating doses of ganetespib and vehicle on the QTc (F) interval (left) and QRS interval (right) in male rabbit hearts. Ganetespib values presented as the mean ($\pm$SEM); $n = 6$, except $n = 2$ at 10^{-8} mol/L and $n = 4$ at 10^{-6} mol/L. No measurements were possible at 10^{-4} mol/L due to arrhythmias. Because of differences in formulation procedure, 4 hearts were perfused with concentrations of 10^{-7} to 10^{-4} mol/L of ganetespib. The remaining 2 hearts were perfused with concentrations of 10^{-8} to 10^{-4} mol/L of ganetespib. Therefore, the vehicle time points in parentheses in the figure correspond to when the 4 test hearts differ from the 2 test hearts. Vehicle values are presented from 1 animal.

ganetespib was derived from diverse tissue origins. Notably, many of the most acutely sensitive lines harbored activating mutations or amplifications of these oncoproteins, including EGFR, c-MET, BCR-ABL, B-RAF, c-KIT, and HER2, consistent with the hypothesis that these oncogenic drivers are more reliant on Hsp90 for their stability and function (35). The *in vitro* activity of ganetespib translated to potent antitumor efficacy in a series of xenograft models selected for their dependence on such oncogenic pathways for growth. In addition, ganetespib exhibited robust cellular potency against drug-resistant tumor phenotypes, overcoming molecular alterations in NSCLC lines that confer clinical resistance to a number of small-molecule TKIs. Furthermore, we discovered that even brief exposure to ganetespib (as little as 5 to 60 minutes) resulted in potent cytotoxic responses in NSCLC cells with IC_{50} values readily achievable *in vivo*. Emerging evidence from the use of small-molecule TKIs in a variety of human cancers indicates that transient, potent oncogene inhibition can be sufficient to induce clinically relevant effects on cellular viability (36, 37). Taken together, these findings strongly indicate that ganetespib is likely to

Published OnlineFirst December 5, 2011; DOI: 10.1158/1535-7163.MCT-11-0755

have broad therapeutic use in a variety of human malignancies and imply that the durable response property of ganetespib may support the use of intermittent dosing schedules in the clinic.

With its unique chemical structure, ganetespib exhibited several key pharmacologic and biologic properties sufficient to account for the potent antitumor responses observed. The compound has relatively high lipophicility that, along with its smaller size, would be expected to facilitate transport across lipid membranes and into cells. In xenograft bearing animals, ganetespib showed selective retention in tumor tissue with similar kinetics as those reported for other resorcinolic Hsp90 inhibitors (38). The most important observation, however, was that the physicochemical properties of the compound resulted in extensive penetration and distribution of ganetespib throughout tumors, including hypoxic regions distal to the nearest blood vessels. From a clinical perspective, the effectiveness of many anticancer agents can be compromised by limited drug distribution, as efficient penetration is necessary to reach the target population and in concentrations sufficient to exert a therapeutic effect (39). In this regard, ganetespib treatment rapidly and dramatically reduced proliferation and induced apoptosis in xenograft tissues independent of the distance from the microvasculature. The capacity of ganetespib to penetrate the extravascular compartment of solid tumors combined with its extended tumor retention and cellular potency clearly predicts for maximal efficacy.

Overall unfavorable safety profiles, including hepatotoxicity, have hampered the clinical application of the ansamycin class of Hsp90 inhibitors. There the chemical reactivity of the benzoquinone group appears accountable for the observed elevation of liver enzymes and associated liver toxicity in the clinical setting (4). Consistent with the findings for other rationally designed second-generation inhibitors, ganetespib showed no evidence of liver toxicity in the preclinical assessment of changes in liver enzymes or histopathology. In addition, cardiac toxicity is a potential risk factor for many classes of drugs, in part, due to adverse effects on critical ion channels that regulate the beating of the heart (37). Our cardiovascular analysis revealed that the 2 predominant effects attributable to exposure to ganetespib in the Langendorff assay were a slight dose-dependent lengthening of the PQ interval and a minor change in QRS duration at the 10^{-5} mol/L concentration. Moreover, the observation that the QTc interval did not lengthen is consistent with ganetespib having no effect on ventricular repolarization. Together with no significant alterations in other electrophysiologic and mechanical parameters, ganetespib, therefore, exhibits a favorable cardiotoxic profile. Importantly, our safety studies were carried out to maximally tolerated doses and no other adverse events were seen to indicate that ganetespib manifests any additional toxicities. Notably, ocular toxicities have recently emerged as an undesirable side-effect for the newer synthetic Hsp90 inhibitors (40). To date, more than 400 patients have been treated with ganetespib, and an absence of ocular toxicity is evident (<3%; W. Ying, unpublished observation). Currently a comprehensive profiling of ganetespib and other Hsp90 inhibitors for potential CNS or ocular toxicity risks is underway.

In summary, we have developed and characterized a unique small-molecule Hsp90 inhibitor that exhibits potent and sustained antitumor effects in a broad range of malignancies both *in vitro* and *in vivo*. Importantly, ganetespib retained its potency against tumor phenotypes that confer drug resistance to agents currently in use in the clinic. In addition, ganetespib displays optimal pharmacologic properties including high tumor penetration and a favorable safety profile that predict for a superior therapeutic index. Accordingly, ganetespib represents an exciting new targeted agent for the treatment of human cancers.

Disclosure of Potential Conflicts of Interest

All authors are current or former employees of Synta Pharmaceuticals Corp.

Acknowledgments

The authors thank Tim Koburt, Donald Smith, Chaohua Zhang, and Yuan Liu for their excellent technical assistance and dedication to the project and Richard Bates who provided drafts and editorial assistance during preparation of the manuscript.

Grant Support

All research work was funded by Synta Pharmaceuticals Corp.

The costs of publication of this article were defrayed in part by the payment of page charges. This article must therefore be hereby marked *advertisement* in accordance with 18 U.S.C. Section 1734 solely to indicate this fact.

Received September 20, 2011; revised November 22, 2011; accepted November 22, 2011; published OnlineFirst December 5, 2011.

References

1. Whitesell L, Lindquist SL. HSP90 and the chaperoning of cancer. Nat Rev Cancer 2005;5:761–72.
2. Solit DB, Rosen N. Hsp90: a novel target for cancer therapy. Curr Top Med Chem 2006;6:1205–14.
3. Trepel J, Mollapour M, Giaccone G, Neckers L. Targeting the dynamic HSP90 complex in cancer. Nat Rev Cancer 2010;10:537–49.
4. Taldone T, Gozman A, Maharaj R, Chiosis G. Targeting Hsp90: small-molecule inhibitors and their clinical development. Curr Opin Pharmacol 2008;8:370–4.
5. da Rocha Dias S, Friedlos F, Light Y, Springer C, Workman P, Marais R. Activated B-RAF is an Hsp90 client protein that is targeted by the anticancer drug 17-allylamino-17-demethoxygeldanamycin. Cancer Res 2005;65:10686–91.
6. Shimamura T, Lowell AM, Engelman JA, Shapiro GI. Epidermal growth factor receptors harboring kinase domain mutations associate with the heat shock protein 90 chaperone and are destabilized following exposure to geldanamycins. Cancer Res 2005;65:6401–8.

Published OnlineFirst December 5, 2011; DOI: 10.1158/1535-7163.MCT-11-0755

7. Workman P. Combinatorial attack on multistep oncogenesis by inhibiting the Hsp90 molecular chaperone. Cancer Lett 2004;206:149–57.
8. Solit DB, Chiosis G. Development and application of Hsp90 inhibitors. Drug Discov Today 2008;13:38–43.
9. Xu W, Neckers L. Targeting the molecular chaperone heat shock protein 90 provides a multifaceted effect on diverse cell signaling pathways of cancer cells. Clin Cancer Res 2007;13:1625–9.
10. Neckers L. Heat shock protein 90: the cancer chaperone. J Biosci 2007;32:517–30.
11. Banerji U. Heat shock protein 90 as a drug target: some like it hot. Clin Cancer Res 2009;15:9–14.
12. Li Y, Zhang T, Schwartz SJ, Sun D. New developments in Hsp90 inhibitors as anti-cancer therapeutics: mechanisms, clinical perspective and more potential. Drug Resist Updat 2009;12:17–27.
13. Banerji U, Judson I, Workman P. The clinical applications of heat shock protein inhibitors in cancer–present and future. Curr Cancer Drug Targets 2003;3:385–90.
14. Powers MV, Workman P. Targeting of multiple signalling pathways by heat shock protein 90 molecular chaperone inhibitors. Endocr Relat Cancer 2006;13:S125–35.
15. Kim YS, Alarcon SV, Lee S, Lee MJ, Giaccone G, Neckers L, et al. Update on Hsp90 inhibitors in clinical trial. Curr Top Med Chem 2009;9:1479–92.
16. Biamonte MA, Van de Water R, Arndt JW, Scannevin RH, Perret D, Lee WC. Heat shock protein 90: inhibitors in clinical trials. J Med Chem 2010;53:3–17.
17. Lundgren K, Zhang H, Brekken J, Huser N, Powell RE, Timple N, et al. BIIB021, an orally available, fully synthetic small-molecule inhibitor of the heat shock protein Hsp90. Mol Cancer Ther 2009;8:921–9.
18. Eccles SA, Massey A, Raynaud FI, Sharp SY, Box G, Valenti M, et al. NVP-AUY922: a novel heat shock protein 90 inhibitor active against xenograft tumor growth, angiogenesis, and metastasis. Cancer Res 2008;68:2850–60.
19. Huang KH, Veal JM, Fadden RP, Rice JW, Eaves J, Strachan JP, et al. Discovery of novel 2-aminobenzamide inhibitors of heat shock protein 90 as potent, selective and orally active antitumor agents. J Med Chem 2009;52:4288–305.
20. Woodhead AJ, Angove H, Carr MG, Chessari G, Congreve M, Coyle JE, et al. Discovery of (2,4-dihydroxy-5-isopropylphenyl)-[5-(4-methylpiperazin-1-ylmethyl)-1,3-dihydroisoindol-2-yl]methanone (AT13387), a novel inhibitor of the molecular chaperone Hsp90 by fragment based drug design. J Med Chem 2010;53:5956–69.
21. Bao R, Lai CJ, Qu H, Wang D, Yin L, Zifcak B, et al. CUDC-305, a novel synthetic HSP90 inhibitor with unique pharmacologic properties for cancer therapy. Clin Cancer Res 2009;15:4046–57.
22. Caldas-Lopes E, Cerchietti L, Ahn JH, Clement CC, Robles AI, Rodina A, et al. Hsp90 inhibitor PU-H71, a multimodal inhibitor of malignancy, induces complete responses in triple-negative breast cancer models. Proc Natl Acad Sci U S A 2009;106:8368–73.
23. Porter JR, Fritz CC, Depew KM. Discovery and development of Hsp90 inhibitors: a promising pathway for cancer therapy. Curr Opin Chem Biol 2010;14:412–20.
24. Proia DA, Foley KP, Korbut T, Sang J, Smith D, Bates RC, et al. Multifaceted intervention by the Hsp90 inhibitor ganetespib (STA-9090) in cancer cells with activated JAK/STAT signaling. PLoS One 2011;6:e18552.
25. Hahn JS. The Hsp90 chaperone machinery: from structure to drug development. BMB Rep 2009;42:623–30.
26. Haber DA, Bell DW, Sordella R, Kwak EL, Godin-Heymann N, Sharma SV, et al. Molecular targeted therapy of lung cancer: EGFR mutations and response to EGFR inhibitors. Cold Spring Harb Symp Quant Biol 2005;70:419–26.
27. Yano S, Wang W, Li Q, Matsumoto K, Sakurama H, Nakamura T, et al. Hepatocyte growth factor induces gefitinib resistance of lung adenocarcinoma with epidermal growth factor receptor-activating mutations. Cancer Res 2008;68:9479–87.
28. Turke AB, Zejnullahu K, Wu YL, Song Y, Dias-Santagata D, Lifshits E, et al. Preexistence and clonal selection of MET amplification in EGFR mutant NSCLC. Cancer Cell 2010;17:77–88.
29. Small D. FLT3 mutations: biology and treatment. Hematology Am Soc Hematol Educ Program 2006;178–84.
30. Lin W, Kao HW, Robinson D, Kung HJ, Wu CW, Chen HC. Tyrosine kinases and gastric cancer. Oncogene 2000;19:5680–9.
31. Dollins DE, Warren JJ, Immormino RM, Gewirth DT. Structures of GRP94-nucleotide complexes reveal mechanistic differences between the hsp90 chaperones. Mol Cell 2007;28:41–56.
32. Krukenberg KA, Street TO, Lavery LA, Agard DA. Conformational dynamics of the molecular chaperone Hsp90. Q Rev Biophys 2011;44:229–55.
33. Richter K, Soroka J, Skalniak L, Leskovar A, Hessling M, Reinstein J, et al. Conserved conformational changes in the ATPase cycle of human Hsp90. J Biol Chem 2008;283:17757–65.
34. Weinstein IB, Joe A. Oncogene addiction. Cancer Res 2008;68:3077–80.
35. Prodromou C. Strategies for stalling malignancy: targeting cancer's addiction to Hsp90. Curr Top Med Chem 2009;9:1352–68.
36. Shah NP, Kasap C, Weier C, Balbas M, Nicoll JM, Bleickardt E, et al. Transient potent BCR-ABL inhibition is sufficient to commit chronic myeloid leukemia cells irreversibly to apoptosis. Cancer Cell 2008;14:485–93.
37. Snead JL, O'Hare T, Adrian LT, Eide CA, Lange T, Druker BJ, et al. Acute dasatinib exposure commits Bcr-Abl-dependent cells to apoptosis. Blood 2009;114:3459–63.
38. Lyons J, Curry J, Smyth T, Harada I, Fazal L, Reule M, et al. Comparison of long-term pharmacodynamic actions of the synthetic small molecule HSP90 inhibitor AT13387 in multiple xenograft models. Mol Cancer Ther 2009;8 Suppl 1:A217.
39. Minchinton AI, Tannock IF. Drug penetration in solid tumours. Nat Rev Cancer 2006;6:583–92.
40. Samuel TA, Sessa C, Britten C, Milligan KS, Mita MM, Banerji U, et al. AUY922, a novel HSP90 inhibitor: final results of a first-in-human study in patients with advanced solid malignancies. J Clin Oncol 28:15s, 2010 (suppl; abstr 2528).

Published OnlineFirst December 5, 2011; DOI: 10.1158/1535-7163.MCT-11-0755

Molecular Cancer Therapeutics

Ganetespib, a Unique Triazolone-Containing Hsp90 Inhibitor, Exhibits Potent Antitumor Activity and a Superior Safety Profile for Cancer Therapy

Weiwen Ying, Zhenjian Du, Lijun Sun, et al.

Mol Cancer Ther 2012;11:475-484. Published OnlineFirst December 5, 2011.